medRxiv preprint doi: https://doi.org/10.1101/2022.03.22.22272760; this version posted March 23, 2022. The copyright holder for this preprint (which was not certified by peer review) is the author/funder, who has granted medRxiv a license to display the preprint in perpetuity. All rights reserved. No reuse allowed without permission.

Ventricular and Atrial Pressure-Volume Loops: Analysis of the Effects Induced by Right Centrifugal Pump Assistance.

Beatrice De Lazzari[1]
[1] "Foro Italico" 4th University of Rome, Italy
beatrice.delazzari@gmail.com

Attilio Iacovoni[2]
[2] ASST-Papa Giovanni XIII Hospital, Bergamo, Italy
aiacovoni@asst-pg23.it

Massimo Capoccia[4,5]
[4]Leeds General Infirmary, Leeds Teaching Hospitals NHS Trust, Leeds, UK
[5]Department of Biomedical Engineering, University of Strathclyde, Glasgow, UK
capoccia@doctors.org.uk

Silvia Papa[6]
[6]Department of Clinical, Internal, Anesthesiology and Cardiovascular Sciences, 'Sapienza' University of Rome, Italy
silvia.papa@uniroma1.it

Roberto Badagliacca[6]
[6]Department of Clinical, Internal, Anesthesiology and Cardiovascular Sciences, 'Sapienza' University of Rome, Italy
roberto.badagliacca@uniroma1.it

Carmine Dario Vizza[6]
[6] Department of Clinical, Internal, Anesthesiology and Cardiovascular Sciences, 'Sapienza' University of Rome dario.vizza@gmail.com

Claudio De Lazzari[7,8]
[7]National Research Council, Institute of Clinical Physiology (IFC-CNR), Rome, Italy
Via Palestro, 32 (00185) Rome, Italy
[8]Teaching University Geomedi, Tbilisi, Georgia
claudio.delazzari@ifc.cnr.it

NOTE: This preprint reports new research that has not been certified by peer review and should not be used to guide clinical practice.

medRxiv preprint doi: https://doi.org/10.1101/2022.03.22.22272760; this version posted March 23, 2022. The copyright holder for this preprint (which was not certified by peer review) is the author/funder, who has granted medRxiv a license to display the preprint in perpetuity. All rights reserved. No reuse allowed without permission.

De Lazzari Claudio

ABSTRACT

Background and Objective: The main indications for right ventricular assist device (RVAD) support are right heart failure after implantation of a left ventricular assist device (LVAD) or early graft failure following heart transplantation. About 30-40% of patients will need RVAD support after LVAD implantation. Pulmonary hypertension is also an indication for right heart assistance. Several types of RVAD generating pulsatile or continuous flow are available on the market. These assist devices can be connected to the cardiovascular system in different ways. We sought to analyse the effects induced by different RVAD connections when right ventricular elastance is modified using a numerical simulator. The analysis was based on the behaviour of both left and right ventricular and atrial loops in the pressure-volume plane.

Methods: New modules of the cardiovascular network and a right ventricular centrifugal pump were implemented in CARDIOSIM© software simulator platform. The numerical pump model generated continuous flow when connected in series or parallel to the right ventricle. When the RVAD was connected in series (parallel), the pump removed blood from the right ventricle (atrium) and ejected it into the pulmonary artery. In our study, we analysed the effects induced by RVAD support on left/right ventricular/atrial loops when right ventricular elastance slope (Ees_{RIGHT}) changed from 0.3 to 0.8 mmHg/ml with the pump connected either in series or parallel. The effect of low and high rotational pump speed was also addressed.

Results: Percentage changes up to 60% were observed for left ventricular pressure-volume area and external work during in-parallel RVAD support at 4000 rpm with Ees_{RIGHT} = 0.3mmHg/ml. The same pump setting and connection type led to percentage

medRxiv preprint doi: https://doi.org/10.1101/2022.03.22.22272760; this version posted March 23, 2022. The copyright holder for this preprint (which was not certified by peer review) is the author/funder, who has granted medRxiv a license to display the preprint in perpetuity. All rights reserved. No reuse allowed without permission.

variation up to 20% for left ventricular ESV and up to 25% for left ventricular EDV with Ees_{RIGHT} = 0.3mmHg/ml. Again the same pump setting and connection generated up to 50% change in left atrial pressure-volume loop area ($PVLA_{L-A}$) and only 3% change in right atrial pressure-volume loop area ($PVLA_{R-A}$) when Ees_{RIGHT} = 0.3mmHg/ml. Percentage variation was lower when Ees_{RIGHT} was increased up to 0.8 mmHg/ml.

Conclusion: Early recognition of right ventricular failure followed by aggressive treatment is desirable to achieve a more favourable outcome. RVAD support remains an option for advanced right ventricular failure although onset of major adverse events may preclude its use.

Key words: Heart failure; RVAD; Pressure-volume loop; Lumped parameter model; Software simulation; Cardiovascular modelling; Rotational pump speed; Right–left heart interaction.

medRxiv preprint doi: https://doi.org/10.1101/2022.03.22.22272760; this version posted March 23, 2022. The copyright holder for this preprint (which was not certified by peer review) is the author/funder, who has granted medRxiv a license to display the preprint in perpetuity. All rights reserved. No reuse allowed without permission.

INTRODUCTION

The main indications for right ventricular assist device (RVAD) support are right heart failure after implantation of a left ventricular assist device (LVAD) or early graft failure following heart transplantation. Measurement of right heart function is often overlooked during daily clinical practice. The study by [1] is an attempt to better understand RV pathophysiology in the setting of pulmonary hypertension, which represents the prevalent pathological condition for RVAD indication, whether to support a failing left ventricle or a primarily involved RV [2].

However, the lack of data does not allow an in-depth analysis of right ventricular and atrial behaviour during RVAD support. An attempt in this direction can be made using a numerical simulator of the cardiovascular system with a view to reproduce pathological conditions requiring right ventricular assistance.

The aim of our study was the analysis of the haemodynamic and energetic variables of both ventricles and atria in different cardiovascular conditions reproduced by changing right ventricular contractility from 0.3 to 0.8 mmHg/ml during RVAD support with different rotational speeds.

The first step of this work required the implementation of two new modules within CARDIOSIM© software simulation platform, which would reproduce the characteristics of the left circulatory network and a continuous flow centrifugal pump (RVAD) to be connected either in series or parallel to the right ventricle. The new modules were based on a 0-D (lumped-parameter) numerical model including input and output cannula of the RVAD.

medRxiv preprint doi: https://doi.org/10.1101/2022.03.22.22272760; this version posted March 23, 2022. The copyright holder for this preprint (which was not certified by peer review) is the author/funder, who has granted medRxiv a license to display the preprint in perpetuity. All rights reserved. No reuse allowed without permission.

We simulated RVAD support following in series and parallel connection driven by different rotational speeds in a heart failure setting. Subsequently, the right ventricular elastance was increased from 0.3 to 0.8 mmHg/ml in a stepwise manner. During each setting, we focused our attention on the following hemodynamic and energetic variables:

- ✓ Right and left ventricular end-systolic volume (ESV_{R-V} and ESV_{L-V});
- ✓ Right and left ventricular end-diastolic volume (EDV_{R-V} and EDV_{L-V});
- ✓ Stroke volume (SV);
- ✓ Right and left ventricular external work (EW_{R-V} and EW_{L-V}) and pressure-volume area (PVA_{R-V} and PVA_{L-V});
- ✓ Right and left atrial end-systolic volume (ESV_{R-A} and ESV_{L-A});
- ✓ Right and left atrial end-diastolic volume (EDV_{R-A} and EDV_{L-A});
- ✓ Right and left atrial pressure-volume loop area ($PVLA_{R-A}$ and $PVLA_{L-A}$);
- ✓ Cardiac output (CO);
- ✓ Systolic, diastolic and mean systemic aortic pressure (AoP);
- ✓ Systolic, diastolic and mean pulmonary arterial pressure (PAP);
- ✓ Pulmonary capillary wedge pressure (PCWP);
- ✓ Right and left atrial pressure (RAP and LAP).

medRxiv preprint doi: https://doi.org/10.1101/2022.03.22.22272760; this version posted March 23, 2022. The copyright holder for this preprint (which was not certified by peer review) is the author/funder, who has granted medRxiv a license to display the preprint in perpetuity. All rights reserved. No reuse allowed without permission.

MATERIAL AND METHODS

The heart and circulatory numerical network

CARDIOSIM© software platform has been previously described [3]-[8]. The modules of the software simulator are: systemic and pulmonary arterial section, systemic and pulmonary venous section and the coronary circulation. Native left and right ventricles, atria and septum reproduce the entire cardiac activity; they are implemented in a single module (Fig. 1) using the time-varying elastance concept [4],[5]. The ventricular, atrial and septal activity is synchronized with the electrocardiographic (ECG) signal [5]. Using the modified time-varying elastance theory, the inter-ventricular septum (IVS) interaction and the instantaneous left and right ventricular pressure can be reproduced by [5],[10]:

$$\begin{cases} P_{lv}(t)=\left[\dfrac{e_{Vsp}(t)\cdot e_{lv}(t)}{e_{lv}(t)+e_{Vsp}(t)}\right]\cdot\left[V_{lv}(t)-V_{lv,0}\right]+\left[\dfrac{e_{lv}(t)}{e_{lv}(t)+e_{Vsp}(t)}\right]\cdot P_{rv}(t)+\left[\dfrac{e_{Vsp}(t)}{e_{lv}(t)+e_{Vsp}(t)}\right]\cdot P_{lv,0} \\ P_{rv}(t)=\left[\dfrac{e_{Vsp}(t)\cdot e_{rv}(t)}{e_{Vsp}(t)+e_{rv}(t)}\right]\cdot\left[V_{rv}(t)-V_{rv,0}\right]+\left[\dfrac{e_{rv}(t)}{e_{Vsp}(t)+e_{rv}(t)}\right]\cdot P_{lv}(t)+\left[\dfrac{e_{Vsp}(t)}{e_{Vsp}(t)+e_{rv}(t)}\right]\cdot P_{rv,0} \end{cases} \quad (1)$$

In the same way, the inter-atrial septum (IAS) interaction and the left and right instantaneous atrial pressure can be reproduced by:

$$\begin{cases} P_{la}(t)=\left[\dfrac{e_{Asp}(t)\cdot e_{la}(t)}{e_{la}(t)+e_{Asp}(t)}\right]\cdot\left[V_{la}(t)-V_{la,0}\right]+\left[\dfrac{e_{la}(t)}{e_{la}(t)+e_{Asp}(t)}\right]\cdot P_{ra}(t)+\left[\dfrac{e_{Asp}(t)}{e_{la}(t)+e_{Asp}(t)}\right]\cdot P_{la,0} \\ P_{ra}(t)=\left[\dfrac{e_{Asp}(t)\cdot e_{ra}(t)}{e_{Asp}(t)+e_{ra}(t)}\right]\cdot\left[V_{ra}(t)-V_{ra,0}\right]+\left[\dfrac{e_{ra}(t)}{e_{Asp}(t)+e_{ra}(t)}\right]\cdot P_{la}(t)+\left[\dfrac{e_{Asp}(t)}{e_{Asp}(t)+e_{ra}(t)}\right]\cdot P_{ra,0} \end{cases} \quad (2)$$

The symbols used in Eqs. (1) and (2) have been listed in Table 1. These features allow the simulation of inter-ventricular and intra-ventricular dyssynchrony [10].

Specific modules of the coronary circulation (Fig. 1) are also available in CARDIOSIM© platform [3].

medRxiv preprint doi: https://doi.org/10.1101/2022.03.22.22272760; this version posted March 23, 2022. The copyright holder for this preprint (which was not certified by peer review) is the author/funder, who has granted medRxiv a license to display the preprint in perpetuity. All rights reserved. No reuse allowed without permission.

For the purposes of our study, we have assembled the cardiovascular network with the new module of the systemic circulation whilst the behavior of the heart is modelled as described in [3],[4]. The systemic venous section [3],[6] and the entire pulmonary circulation [7],[8],[11],[12] are modelled as described in current literature. We have selected the module presented in [13] for the coronary circulation. The tricuspid, mitral, pulmonary, and aortic valves are modelled with an ideal diode: when the pressure across the valve is positive, the valve opens and allows the flow of blood; when the pressure is less than or equal to zero, the valve is closes and the flow of blood is zero [3]-[5],[14]

New lumped-parameter model of the systemic circulation

The new module is described in Fig. 1 using resistance, inertance and compliance (RLC) elements. The systemic network consists of the following compartments: ascending and descending aorta, carotid artery, peripheral arteries and superior and inferior vena cava (Fig. 1a).

The ascending (descending) aorta is modelled using two resistances R_{AA} and R_{Vaa} (R_{DA} and R_{Vda}), inertance L_{AA} (L_{DA}) and compliance C_{AA} (C_{DA}). A single resistance (R_{CA}) reproduces the behavior of the carotid district. The peripheral arterial circulation is reproduced with resistances R_A and R_{Va} and with compliance C_A (Fig. 1b). The superior vena cava compartment consists of resistances R_{SVC_I} and R_{SVC_II}, inertance L_{SVC} and compliance C_{SVC}. The systemic venous network is implemented using compliance C_{VS} and resistances R_{VS} and R_{Vvs} (Fig. 1a). Finally, the inferior vena cava district is modelled with resistances R_{IVC}, R_{IVC_I} and R_{IVC_II}, inertance L_{IVC} and compliance C_{IVC} (Fig. 1a). The resistances R_{Vaa}, R_{Vda}, R_{Va}, and R_{Vvs} account for viscous losses of the vessel wall. Pt is the mean intrathoracic pressure.

medRxiv preprint doi: https://doi.org/10.1101/2022.03.22.22272760; this version posted March 23, 2022. The copyright holder for this preprint (which was not certified by peer review) is the author/funder, who has granted medRxiv a license to display the preprint in perpetuity. All rights reserved. No reuse allowed without permission.

Right ventricular assist device (RVAD)

A 0-D numerical model described in [7] was used to implement a centrifugal pump that reproduced the behavior of the right ventricular assist device. The pump can be connected in series or parallel to the right ventricle with two cannulae modelled using RLC elements (Fig. 1c). When the RVAD removes blood from the right atrium (parallel connection – SW1=ON and SW2=OFF in Fig. 1c), the flow through the inlet cannula is:

$$\left(RAP - \Delta P\right) = Qi_{CANN} \cdot Ri_{CANN} + \left(\frac{d}{dt} Qi_{CANN}\right) \cdot Li_{CANN} \tag{3}$$

$$\left(\frac{d}{dt}\Delta P\right) \cdot Ci_{CANN} = Q_{PUMP} - Qi_{CANN} \tag{4}$$

RAP is the right atrial pressure, $Li_{CANN,}$ Ri_{CANN} and Ci_{CANN} are the inertance, resistance and compliance of the inlet cannula, respectively (Fig 1c). Qi_{CANN} (Q_{PUMP}) is the flow through the inlet cannula (generated by the centrifugal pump). ΔP is the pressure on the pump head.

When the RVAD removes blood from the right ventricle (in series connection - SW1=OFF and SW2=ON in Fig. 1c), Eq. 3 becomes:

$$\left(RVP - \Delta P\right) = Qi_{CANN} \cdot Ri_{CANN} + \left(\frac{d}{dt} Qi_{CANN}\right) \cdot Li_{CANN} \tag{5}$$

RVP is the right ventricular pressure.

When the RVAD ejects blood, the flow through the outlet cannula is:

$$\left(\Delta P - MPAP\right) = Qo_{CANN} \cdot Ro_{CANN} + \left(\frac{d}{dt} Qo_{CANN}\right) \cdot Lo_{CANN} \tag{6}$$

$$\left(\frac{d}{dt}\Delta P\right) \cdot Co_{CANN} = Qo_{PUMP} - Qo_{CANN} \tag{7}$$

medRxiv preprint doi: https://doi.org/10.1101/2022.03.22.22272760; this version posted March 23, 2022. The copyright holder for this preprint (which was not certified by peer review) is the author/funder, who has granted medRxiv a license to display the preprint in perpetuity. All rights reserved. No reuse allowed without permission.

MPAP is the mean pulmonary artery pressure (Fig. 1c), Ro_{CANN} and Co_{CANN} are the inertance, resistance and compliance of the outlet cannula, respectively. Qo_{CANN} is the flow through the outlet cannula.

Simulation Protocol

For the purposes of our simulations, we considered values for right and left ventricular elastance that could reproduce a realistic diseased heart. According to the available literature, normal values for right ventricular elastance fluctuate around 1 mmHg/ml [15],[16] and range from 1.6 to 5 mmHg/ml for left ventricular elastance [17],[18]. Therefore, we considered Ees_{LEFT} = 0.7 mmHg/ml for the left ventricle and Ees_{RIGHT} = 0.3 mmHg/ml for the right ventricle as reference values for a failing heart. Our simulation approach consisted of three steps. In the first step after setting HR= 90 bpm, the slope of left ventricular End-Systolic Pressure-Volume Relationship (ESPVR) Ees_{LEFT}=0.7 mmHg/ml and the slope of right ESPVR Ees_{RIGHT}=0.3 mmHg/ml [8], the simulator generated the following values: cardiac output (CO) 4.51 l/min, aortic systolic (diastolic) pressure 82.1 (60.4) mmHg, mean right atrial pressure 23.3 mmHg, pulmonary systolic (diastolic) pressure 51.2 (31.6) mmHg and pulmonary capillary wedge pressure 20.7 mmHg. The mean pressure (flow) value was calculated as the mean value of all blood pressure (flow) measurements during a cardiac cycle.

In the second step, the slope of right ESPVR Ees_{RIGHT}=0.3 mmHg/ml was set to 0.4, 0.5, 0.6, 0.7 and 0.8 mmHg/ml [1],[19] and for each value the parameters described above were measured.

In the third step, RVAD support was applied both in series and parallel mode with rotational speed of 2000, 2500, 3000, 3500 and 4000 rpm. In the fourth step, the slope of

medRxiv preprint doi: https://doi.org/10.1101/2022.03.22.22272760; this version posted March 23, 2022. The copyright holder for this preprint (which was not certified by peer review) is the author/funder, who has granted medRxiv a license to display the preprint in perpetuity. All rights reserved. No reuse allowed without permission.

right ESPVR was changed from 0.3 to 0.8 mmHg/ml (0.1 mmHg/ml stepwise increase) during RVAD support connected in series and parallel mode. The measured parameters were those described above.

Considering that we did not measure data in patients undergoing RVAD support to allow us to reproduce their haemodynamic conditions with our numerical simulator, and given that literature data are largely incomplete, we decided against a direct data comparison. Therefore, we considered percentage variation to evaluate the trend of the effects induced by RVAD support on the haemodynamic and energetic variables in line with other available simulation work.

medRxiv preprint doi: https://doi.org/10.1101/2022.03.22.22272760; this version posted March 23, 2022. The copyright holder for this preprint (which was not certified by peer review) is the author/funder, who has granted medRxiv a license to display the preprint in perpetuity. All rights reserved. No reuse allowed without permission.

RESULTS

Figure 2 shows the effects induced by different values for ESPVR slope (Ees_{RIGHT}) on left and right atrial pressure-volume loop area (left upper panel). The percentage changes calculated with respect to the reference value for Ees_{RIGHT}=0.3 mmHg/ml have been listed. The red bars show the percentage change with respect to the reference value for $PVLA_{L-A}$ increase at high Ees_{RIGHT} values. On the contrary, the $PVLA_{R-A}$ (yellow bars) decreases when the percentage change is referred to high Ees_{RIGHT} values. These results show that when Ees_{RIGHT} increases from 0.3 to 08 mmHg/ml, the area of the pressure-volume loop of the right atrium decreases whilst the area of the pressure-volume loop of the left atrium increases (Fig. 3). The left and right lower panel shows the left and right atrial pressure-volume loop obtained with different Ees_{RIGHT} values. The black pressure-volume loop was obtained setting Ees_{RIGHT}=0.3 mmHg/ml, while the blue pressure-volume loop was obtained setting Ees_{RIGHT}=0.6 mmHg/ml. The left (left side) and the right (right side) ventricular pressure-volume loops are placed in the upper panels. When Ees_{RIGHT} increases, EW_{L_V} and PVA_{L-V} (left upper panel) increase leading to right-sided shift with increased left ESV and EDV. The effect induced by different Ees_{RIGHT} values on left and right ventricular EW (EW_{L-V} and EW_{R-V}) are reported in Fig. 2 (left lower panel). The effect induced on EDV and ESV of the left (right) atrium is reported in the upper (lower) right panel (Fig. 2). The effect induced on right atrial ESV is more evident than the one produced on right atrial EDV. Figure 3 (right upper panel) shows that an increase in Ees_{RIGHT} leads to an increase in right ventricular external work and PVA_{R-V} with left-sided shift and decrease of both right ESV and EDV. Figure 4 shows the effect induced by RVAD support driven in parallel connection (left panels) on left ventricular

medRxiv preprint doi: https://doi.org/10.1101/2022.03.22.22272760; this version posted March 23, 2022. The copyright holder for this preprint (which was not certified by peer review) is the author/funder, who has granted medRxiv a license to display the preprint in perpetuity. All rights reserved. No reuse allowed without permission.

PVA_{L-V} (left upper panel) and EW_{L-V} (left lower panel). The effect induced on PVA_{L-V} and EW_{L-V} when the RVAD is driven in series is available in the right panels. The data were measured for different values of Ees_{RIGHT} (0.3; 0.5 and 0.8 mmHg/ml) and with increasing RVAD rotational speed (2000; 2500; 3000; 3500 and 4000 rpm). For each rotational speed and Ees_{RIGHT} values, the percentage changes calculated with respect to the reference value measured in pathological conditions have been listed (Fig. 4). The highest percentage changes in PVA_{L-V} and EW_{L-V} (50% or more for both variables) were recorded in a diseased condition with right ventricular elastance set to Ees_{RIGHT}=0.3 mmHg/ml during in-parallel RVAD assistance with pump rotational speed at 4000 rpm. Figure 5 shows the effect induced by in-parallel RVAD support on left ventricular ESV_{L-V} (left upper panel) and EDV_{L-V} (left lower panel). The effect induced on ESV_{L-V} (right upper panel) and EDV_{L-V} (right lower panel) by in-series RVAD support is also available for comparison purposes. When the rotational speed of the pump was set to 2000 rpm, the percentage changes for each value of right ventricular ESPVR slope were no more than 3%. The effects induced by different rotational speed of the RVAD on left and right atrial pressure-volume loop area are available in Fig. 6 for three different values of right ESPVR slope. In addition, for each value of the slope, the effect induced by the pump has been calculated in percentage terms with respect to the value obtained without assistance. In the case of the right atrium, we observed a higher percentage reduction of the loop area (from 2% to 9%) during in-series assistance (left lower panel). In the case of parallel connection (left upper panel), the percentage reduction of the pressure-volume loop area of the right atrium becomes more evident at high values for both the slope and the pump rotational speed. Right heart assistance produces significant effects on the left atrium

medRxiv preprint doi: https://doi.org/10.1101/2022.03.22.22272760; this version posted March 23, 2022. The copyright holder for this preprint (which was not certified by peer review) is the author/funder, who has granted medRxiv a license to display the preprint in perpetuity. All rights reserved. No reuse allowed without permission.

loop area (right panels). Percentage variations between 20% and 50% are observed when the RVAD is connected in parallel to the right ventricle (right upper panel). Whether in-series or in-parallel assistance is considered, the most significant percentage variations are observed when the right ventricular ESPVR slope is set to Ees_{RIGHT}=0.3 mmHg/ml.

The effects induced by RVAD support on the right ventricular flow output and on the total cardiac output are showed in Fig. 7. RVAD parallel assistance generated a lower reduction in right ventricular output compared to in series assistance for each Ees_{RIGHT} value and each pump rotational speed. More specifically, when the pump speed was set to 4000 rpm, parallel assistance induced a reduction between 20% and 45% compared to the baseline value while the in series assistance induced a reduction between 38% and 78%. The upper panels in Fig. 7 show that parallel RVAD assistance generates a higher increase in total cardiac output compared to in series assistance at pump speeds higher than 3500 rpm (for each Ees_{RIGHT} value).

The left upper (lower) panel in Fig. 8 shows the effects induced on left ventricular (atrial) loop when different types of RVAD assistance were applied to pathological conditions (black loops) reproduced by setting Ees_{RIGHT} to 0.3 mmHg/ml. The assistance was applied in parallel (red loops) and in series (blue loops) mode with rotational speed of 3000 rpm.

The right upper (lower) panel shows the effects induced on right ventricular (atrial) loops. When in-parallel assistance was applied, a right-sided shift in the left and right ventricular loop (red lines) was observed. Although in-series RVAD assistance did not cause changes in right end-systolic ventricular volume, it leaded to a reduction in right

medRxiv preprint doi: https://doi.org/10.1101/2022.03.22.22272760; this version posted March 23, 2022. The copyright holder for this preprint (which was not certified by peer review) is the author/funder, who has granted medRxiv a license to display the preprint in perpetuity. All rights reserved. No reuse allowed without permission.

end-diastolic ventricular loop. The type of assistance did not cause relevant changes in the right atrial loop (right lower panel).

medRxiv preprint doi: https://doi.org/10.1101/2022.03.22.22272760; this version posted March 23, 2022. The copyright holder for this preprint (which was not certified by peer review) is the author/funder, who has granted medRxiv a license to display the preprint in perpetuity. All rights reserved. No reuse allowed without permission.

DISCUSSION

The left ventricle (LV) is coupled to the low-compliance, high-resistance peripheral arterial circulation and is more adaptable to changes in pressure than volume. In contrast, the right ventricle (RV) is coupled to the high-compliance, low-resistance pulmonary circulation and is more adaptable to changes in volume than pressure. The right ventricle consists of a free wall containing a wrap-around circumferential muscle at its base and a septum made of oblique helical fibres crossing each other at 60° angles. This is consistent with the helical ventricular myocardial band concept, which defines two interconnected muscle bands: a basal loop with transverse fibres surrounding the left and right ventricles and an apical loop made of a right- and left-handed helix forming an apical vortex [20],[21]. The wrap-around transverse fibres constrict or compress leading to a bellows motion responsible for 20% of right ventricular output whilst the oblique fibres are responsible for shortening and lengthening, which contribute to 80% of right ventricular systolic function [22]. The crista supra-ventricularis shares muscle fibers with the inter-ventricular septum and the free wall playing a key anatomical and functional role [23]. A reduction in longitudinal contraction and an increase in transverse shortening are observed following cardiopulmonary bypass and pericardiotomy [24]. This is quite an important aspect to bear in mind and may be addressed initially with pulmonary vasodilators [25]. The relationship between structure and function plays a key role in clinical decision-making, which must be based on detailed knowledge of normality and recognise how disease can be addressed to restore normality [22]. The important contribution of right ventricular function has been neglected for a long time due to previous observations and assumptions. The onset of right ventricular dysfunction should

medRxiv preprint doi: https://doi.org/10.1101/2022.03.22.22272760; this version posted March 23, 2022. The copyright holder for this preprint (which was not certified by peer review) is the author/funder, who has granted medRxiv a license to display the preprint in perpetuity. All rights reserved. No reuse allowed without permission.

trigger the search for the main underlying cause in relation to pressure overload, volume overload or primary myocardial disease [26]. Right heart failure (RHF) is difficult to manage because of its complex geometry and a lack of specific treatments aimed at stabilisation and recovery of right ventricular function. Nevertheless, right ventricular dysfunction remains associated with poor clinical outcome regardless of the underlying disease mechanism [27].

A simulation approach overcomes ethical issues and the risk of offering an ineffective or potentially dangerous therapeutic option. At the same time, it may help focus on the specific problem to address. Our starting point was to develop a failing right heart, which would require support at a subsequent stage. The easier way to do it was to act on the ESPVR slope of both ventricles. A range between 0.35 and 0.74 mmHg/ml is observed in patients with pulmonary hypertension [1] with a cut-off of 0.8 for E_{es}/E_a ratio as the onset of right ventricular maladaptation. Our initial aim was to observe the effects of RVAD support with either in series or parallel connection following stepwise variation of right ventricular end-systolic elastance in patients with increased right ventricular afterload. Therefore, the right ventricular end-systolic elastance considered in the present study ranged between 0.3 and 0.8 mmHg/ml as per previously reported values observed in clinical practice [1],[28],[29]. According to [19], increased native cardiac output is observed in the presence of left ventricular systolic impairment when right ventricular end-systolic elastance increases from 0.1 to 1.0 mmHg/ml. An increased native cardiac output is still observed during VA ECMO support following stepwise increase in right ventricular end-systolic elastance but to a lesser degree. A left-to-right ventricular septal shift is observed during diastole following a stepwise increase in right ventricular end-

medRxiv preprint doi: https://doi.org/10.1101/2022.03.22.22272760; this version posted March 23, 2022. The copyright holder for this preprint (which was not certified by peer review) is the author/funder, who has granted medRxiv a license to display the preprint in perpetuity. All rights reserved. No reuse allowed without permission.

systolic elastance both with and without VA ECMO support. Our considerations are based in the context of pure RVAD support with either in series or parallel connection.

PVA and EW of the left ventricle gain benefit when the pump speed of the RVAD is at least 3500 rpm. The highest effect is obtained when Ees_{RIGHT} is 0.3 mmHg/ml, which is consistent with significant RV dysfunction (left panels in Fig. 4). The pathological range considered would suggest that early recognition and aggressive RVAD support is advisable where a lower degree of assistance is required generating enough benefit for a less compromised right ventricle with more potential for recovery. This is an important point to consider in the context of LVAD support when the right heart shows signs of failure requiring attention.

The highest beneficial effect is obtained when the RVAD is connected in parallel to the right ventricle with up to nearly 35% increase in total cardiac output (right upper panel in Fig. 7) and lower reduction of right ventricular output compared to in series RVAD connection. No significant effect is observed on the right atrium regardless the type of RVAD connection to the right ventricle. Instead, in-parallel RVAD connection has a more beneficial effect on the left atrium. Again, RVAD support has a more beneficial effect on ESV and EDV of the left ventricle when connected in parallel to the right ventricle (left panels in Fig. 5). The role of the inter-ventricular septum is critical in this context.

Our aim was to observe the effect of pure RVAD assistance at different stages of right ventricular dysfunction to determine appropriate timing for intervention. Our target was early graft failure secondary to right heart dysfunction following orthotopic heart transplant and right ventricular failure following LVAD insertion in an apparently

medRxiv preprint doi: https://doi.org/10.1101/2022.03.22.22272760; this version posted March 23, 2022. The copyright holder for this preprint (which was not certified by peer review) is the author/funder, who has granted medRxiv a license to display the preprint in perpetuity. All rights reserved. No reuse allowed without permission.

preserved right heart function preoperatively. We have focused our attention mainly on Ees_{RIGHT} neglecting Vo. We have not considered the progressive increase in afterload. Despite these limitation, our preliminary findings support the concept of early intervention in the presence of a failing right heart regardless of its aetiology. This simulation study confirms what had been previously advocated but not always put into practice [30]. A more liberal right ventricular support may be the way forward [31] when considering different support strategies for a failing right ventricle [32]. Late onset of right ventricular failure remains associated with worse survival and higher cumulative incidence of major adverse events [33].

medRxiv preprint doi: https://doi.org/10.1101/2022.03.22.22272760; this version posted March 23, 2022. The copyright holder for this preprint (which was not certified by peer review) is the author/funder, who has granted medRxiv a license to display the preprint in perpetuity. All rights reserved. No reuse allowed without permission.

CONCLUSION

Although RVAD support may be effective in advanced right heart failure, intervention at an earlier stage may require a lesser degree of assistance and be more beneficial for the left ventricle. Early recognition of right ventricular failure followed by aggressive treatment is desirable to achieve a more favourable outcome. RVAD support remains an option for advanced right ventricular failure although the onset of major adverse events may preclude its use. In-parallel RVAD connection to the right ventricle seems a more suitable option.

medRxiv preprint doi: https://doi.org/10.1101/2022.03.22.22272760; this version posted March 23, 2022. The copyright holder for this preprint (which was not certified by peer review) is the author/funder, who has granted medRxiv a license to display the preprint in perpetuity. All rights reserved. No reuse allowed without permission.

De Lazzari Claudio

FUNDING AND CONFLICT OF INTEREST

None

ACKNOWLEDGEMENTS

None

medRxiv preprint doi: https://doi.org/10.1101/2022.03.22.22272760; this version posted March 23, 2022. The copyright holder for this preprint (which was not certified by peer review) is the author/funder, who has granted medRxiv a license to display the preprint in perpetuity. All rights reserved. No reuse allowed without permission.

REFERENCES

[1] K. Tello, A. Dalmer, J. Axmann, R. Vanderpoo, H.A. Ghofrani, R. Naeije, F. Roller, W. Seeger, N. Sommer, J. Wilhelm, H. Gall, M.J. Richter, Reserve of Right Ventricular – Arterial Coupling in the Setting of Chronic Overload. Circ. Heart Fail. 12 (2019) e005512.

[2] M. Arrigo, L.C. Huber, S. Winnik, F. Mikulicic, F. Guidetti, M. Frank, A.J. Flammer, F. Ruschitzka, Right Ventricular Failure: Pathophysiology, Diagnosis and Treatment. Card. Fail. Rev. 5(3) (2019) 140-146.

[3] C. De Lazzari, D. Stalteri. 2011-2019, CARDIOSIM© Website. Original website platform regarding the implementation of the cardiovascular software simulator CARDIOSIM©. (https://cardiosim.dsb.cnr.it/).

[4] C. De Lazzari, et al., Interactive simulator for e-Learning environments: a teaching software for health care professionals, BioMedical Engineering OnLine. 13 (2014) 172.

[5] C. De Lazzari, Interaction between the septum and the left (right) ventricular free wall in order to evaluate the effects on coronary blood flow: numerical simulation, Comput. Methods Biomech. Biomed. Eng. 15(12) (2012) 1359-1368.

[6] M. Capoccia, S. Marconi, S.A. Singh, et al., Simulation as a preoperative planning approach in advanced heart failure patients. A retrospective clinical analysis, BioMedical Engineering OnLine. 17(1) (2018) 52.

[7] B. De Lazzari, A. Iacovoni, K. Mottaghy, M. Capoccia, R. Badagliacca, C.D. Vizza and C. De Lazzari. ECMO Assistance During Mechanical Ventilation: Effects Induced on Energetic and Haemodynamic Variables, Computer Methods and Programs in Biomedicine 202 (2021) 1-13.

[8] C. De Lazzari, B. De Lazzari, A. Iacovoni, S. Marconi, S. Papa, M. Capoccia, S. Papa, R. Badagliacca, C.D. Vizza. Intra-Aortic Balloon Counterpulsation Timing: A New Numerical Model for Programming and Training in the Clinical Environment, Computer Methods and Programs in Biomedicine 194 (2020) 1-9.

[9] S. Marconi, M. Capoccia and C. De Lazzari. Mathematical Modelling of the Cardiovascular System, In: M. Capoccia and C. De Lazzari (Eds) Concepts, Mathematical Modelling and Applications in Hart Failure. Nova Science Publisher, New York, 2019 119-158.

[10] C. De Lazzari. Interaction between the septum and the left (right) ventricular free wall in order to evaluate the effects on coronary blood flow: numerical simulation, Computer Methods in Biomechanics and Biomedical Engineering 15(12) (2012) 1359-1368.

medRxiv preprint doi: https://doi.org/10.1101/2022.03.22.22272760; this version posted March 23, 2022. The copyright holder for this preprint (which was not certified by peer review) is the author/funder, who has granted medRxiv a license to display the preprint in perpetuity. All rights reserved. No reuse allowed without permission.

[11] M. Capoccia, S. Marconi and C. De Lazzari. Decision-making in advanced heart failure patients requiring LVAD insertion: Can preoperative simulation become the way forward? A case study, Journal of Biomedical Engineering and Informatics 4(2) (2018) 8-20. https://doi.org/10.5430/jbei.v4n2p

[12] C. De Lazzari, D. Stalteri. 2011-2019, CARDIOSIM© Website. https://cardiosim.dsb.cnr.it/CirculationModels/pci4

[13] C. De Lazzari, D. Stalteri. 2011-2019, CARDIOSIM© Website. https://cardiosim.dsb.cnr.it/CirculationModels/ncm2

[14] J.T. Ottesen, M. Danielsen, The heart in Mathematical Modelling in Medicine, IOS Press (2000) 1-235

[15] L.J. Dell'Italia, R.A. Walsh. Application of a time varying elastance model to right ventricular performance in man, Cardiovasc. Res. 22 (1988) 864-874.

[16] S. Brimioulle, P. Wauthy, P. Ewalenko, B. Rondelet, F. Vermeulen, F. Kerbaul, R. Naeije. Single-beat estimation of right ventricular end-systolic pressure-volume relationship, Am. J. Physiol. Heart Circ. Physiol. 284 (2003) H1625-H1630.

[17] M.R. Starling. Left ventricular-arterial coupling relations in the normal human heart, Am. Heart J. 125 (1993) 1659-1666.

[18] A. Kiani, J. Gilani Shakibi. Normal Values of Left Ventricular End-Systolic Elastance in Infants and Children, Iran J. Med. Sci. 28(4) (2003) 169-172.

[19] D.W. Donker, M. Sallismani, M.Bromé. Right–Left Ventricular Interaction in Left-Sided Heart Failure With and Without Venoarterial Extracorporeal Membrane Oxygenation Support—A Simulation Study, ASAIO J. 67 (2021) 297-305.

[20] M.J. Kocica, A.F. Corno, F. Carreras-Costa, M. Ballester-Rodes, M.C. Moghbel, C.N. Cueva, et al. The helical ventricular myocardial band: global, three-dimensional, functional architecture of the ventricular myocardium, Eur. J. Cardiothorac. Surg. 29(1) (2006) S21-S40.

[21] G. Buckberg, J.I.E. Hoffman, A. Mahajan, S. Saleh, C. Coghlan. Cardiac mechanics revisited: the relationship of cardiac architecture to ventricular function, Circulation 118 (2008) 2571-2587.

[22] G. Buckberg, J.I.E. Hoffman. Right ventricular architecture responsible for mechanical performance: Unifying the role of ventricular septum, J. Thorac. Cardiovasc. Surg. 148 (2014) 3166-3171.

medRxiv preprint doi: https://doi.org/10.1101/2022.03.22.22272760; this version posted March 23, 2022. The copyright holder for this preprint (which was not certified by peer review) is the author/funder, who has granted medRxiv a license to display the preprint in perpetuity. All rights reserved. No reuse allowed without permission.

[23] T.N. James. Anatomy of the Crista Supraventricularis: Its Importance for Understanding Right Ventricular Function, Right Ventricular Infarction and Related Conditions, J. Am. Coll. Cardiol. 6(5) (1985) 1083-1095.

[24] A. Raina, A. Vaidya, Z.M. Gertz, S. Chambers, P.R. Forfia. Marked changes in right ventricular contractile pattern after cardiothoracic surgery: Implications for post-surgical assessment of right ventricular function, J. Heart Lung Transplant. 32(8) (2013) 777-783.

[25] S.B. Brown, A. Raina, D. Katz, M. Szerlip, S.E. Wiegers, P.R. Forfia. Longitudinal Shortening Accounts for the Majority of Right Ventricular Contraction and Improves After Pulmonary Vasodilator Therapy in Normal Subjects and Patients With Pulmonary Arterial Hypertension, Chest 140(1) (2011) 27-33.

[26] J. Sanz, D. Sánchez-Quintana, E. Bossone, H.I. Bogaard, R. Naeije. Anatomy, Function and Dysfunction of the Right Ventricle, J. Am. Coll. Cardiol. 73(12) (2019) 1463-1482.

[27] M.A. Konstam, M.S. Kiernan, D. Bernstein, B. Bozkurt, M. Jacob, N.K. Kapur, R.D. Kociol, E.F. Lewis, M.R. Mehra, F.D. Pagani, A.N. Raval, C. Ward. On behalf of the American Heart Association Council on Clinical Cardiology; Council on Cardiovascular Disease in the Young; and Council on Cardiovascular Surgery and Anaesthesia. Evaluation and Management of Right-Sided Heart Failure. A Scientific Statement From the American Heart Association. Circulation 137 (2018) e578-e622.

[28] F. Haddad, S.A. Hunt, D.N. Rosenthal, D.J. Murphy. Right Ventricular Function in Cardiovascular Disease, Part I. Anatomy, Physiology, Aging and Functional Assessment of the Right Ventricle, Circulation 117 (2008) 1436-1448.

[29] T. Kuehne, S. Yilmaz, P. Steendijk, P. Moore, M. Groenink, M. Saaed, et al. Magnetic Resonance Imaging Analysis of Right Ventricular Pressure-Volume Loops. In Vivo Validation and Clinical Application in Patients With Pulmonary Hypertension, Circulation 110 (2004) 2010-2016.

[30] J.R. Fitzpatrick, J.R. Frederick, W. Hiesinger, et al. Early planned institution of biventricular mechanical circulatory support results in improved outcomes compared with delayed conversion of a left ventricular assist device to a biventricular assist device, J. Thorac. Cardiovasc. Surg. 137(4) (2009) 971-977.

[31] Q. Fischer, M. Kirsch. Liberal Right Ventricular Assist Device Extracorporeal Membrane Oxygenation Support for Right Ventricular Failure after Implantable Left Ventricular Assist Device Placement, ASAIO J. 64(6) (2018) 741-747.

[32] J.P Beller, J. Hunter Mehaffey, Z.K. Wegermann, M. Grau-Sepulveda, et al. Strategies for Mechanical Right Ventricular Support during Left Ventricular Assist

medRxiv preprint doi: https://doi.org/10.1101/2022.03.22.22272760; this version posted March 23, 2022. The copyright holder for this preprint (which was not certified by peer review) is the author/funder, who has granted medRxiv a license to display the preprint in perpetuity. All rights reserved. No reuse allowed without permission.

Device Implant, Ann. Thorac. Surg. (2021), doi: https://doi.org/10.1016/j.athoracsur.2021.10.032.

[33] J.E. Rame, F.D. Pagani, M.S. Kiernan, G.H. Oliveira, E.Y. Birati, P. Atluri, A. Gaffey, et al. Evolution of Late Right Heart Failure With Left Ventricular Assist Devices and Association With Outcomes, J. Am. Coll. Cardiol. 78 (23) (2021) 2294-2308.

medRxiv preprint doi: https://doi.org/10.1101/2022.03.22.22272760; this version posted March 23, 2022. The copyright holder for this preprint (which was not certified by peer review) is the author/funder, who has granted medRxiv a license to display the preprint in perpetuity. All rights reserved. No reuse allowed without permission.

Figure Captions List

Fig. 1 Electric analogue of the cardiovascular system. The network is assembled with septum, left and right heart, main and small pulmonary arterial sections, pulmonary arteriole and capillary sections, pulmonary venous section. The left circulation include ascending and descending aorta compartments, peripheral arteries and carotid artery sections, coronary circulation, superior and inferior vena cava sections and systemic veins compartment. RVAD is the right ventricular assist device. Table 2 lists the symbols used.

Fig. 1a The behavior of the ascending aorta is simulated with resistances R_{AA} and R_{Vaa}, inertance L_{AA} and compliance C_{AA}. QR_{AA} is the flow through the resistance and inertance. The descending aorta is implemented with resistances R_{DA} and R_{Vda}, inertance L_{DA} and compliance C_{DA}. QR_{DA} is the flow through the resistance (R_{DA}) and inertance (L_{DA}). The carotid arteries section is reproduced with a simple resistance (R_{CA}). The superior vena cava module consists of resistances R_{SVC_I} and R_{SVC_II}, inertance L_{SCV} and compliance C_{SVC}. The inferior vena cava module is modelled with resistances R_{IVC}, R_{IVC_I} and $_{RIVC\_II}$, inertance L_{IVC} and compliance C_{IVC}. The intrathoracic pressure (Pt) affects compliances C_{AA}, C_{DA}, C_{IVC} and C_{SVC}. Table 2 lists the symbols used.

Fig. 1b The peripheral arteries module is modelled with resistances R_A and R_{Va} and compliance C_A. The resistor R_{Va} account for viscous losses of the

medRxiv preprint doi: https://doi.org/10.1101/2022.03.22.22272760; this version posted March 23, 2022. The copyright holder for this preprint (which was not certified by peer review) is the author/funder, who has granted medRxiv a license to display the preprint in perpetuity. All rights reserved. No reuse allowed without permission.

vessels wall. QR_A is the blood flow outside the compartment; it is a part of the blood that reaches the systemic veins compartment.

Fig. 1c Schematic representation of RVAD connection. When the right ventricular assist device is connected in parallel, blood is removed from the right atrium (SW_1=ON and SW_2=OFF) and ejected into the pulmonary artery. When RVAD is connected in series, blood is removed from the right ventricle (SW_1=OFF and SW_2=ON) and ejected into the pulmonary artery. The input (output) RVAD cannula is modelled with RLC elements. Q_{oPUMP} (Q_{iPUMP}) is the output (inlet) flow rate from the pump. Q_{oCANN} (Q_{iCANN}) is the output (inlet) flow rate from the cannula. The electrical analogue of the pulmonary circulation is described in **Error! Reference source not found.**.

Fig.2 Relative changes calculated in comparison to Ees_{RIGHT}=0.3 mmHg/ml for different Ees_{RIGHT} values (0.4-0.8 mmHg/ml). The relative changes of the pressure-volume loop area of the left and right atrium (external work of the left and right ventricle) are reported in the left upper (lower) panel. The right upper (lower) panel shows the relative changes of left (right) atrial end systolic and end diastolic volume.

Fig. 3 Screen output from CARDIOSIM© software simulator. The left (right) upper panel shows four left (right) ventricular pressure-volume loops obtained setting EesR□Ees_{RIGHT}=0.3 mmHg/ml (black line), EesR□Ees_{RIGHT}=0.4 mmHg/ml (green line), EesR□Ees_{RIGHT}=0.5 mmHg/ml (red line) and EesR□Ees_{RIGHT}=0.6 mmHg/ml (blue line)

medRxiv preprint doi: https://doi.org/10.1101/2022.03.22.22272760; this version posted March 23, 2022. The copyright holder for this preprint (which was not certified by peer review) is the author/funder, who has granted medRxiv a license to display the preprint in perpetuity. All rights reserved. No reuse allowed without permission.

respectively. The left (right) lower panel shows four left (right) atrial pressure-volume loops obtained changing the slope of the right ventricular elastance as previously described.

Fig. 4 Relative changes calculated in comparison to pathological conditions (EesR Ees$_{RIGHT}$=0.3; 0.5 and 0.8 mmHg/ml) for different type of RVAD connection and different rotational speed. For each values of Ees$_{RIGHT}$, the relative change was calculated when the RVAD was connected in parallel and in series. The left upper (lower) panel shows the relative changes in the left ventricular pressure-volume area (external work) when the RVAD was connected in parallel to the right ventricle. The right upper (lower) panel shows the relative changes in the left ventricular pressure-volume area (external work) when the RVAD was connected in series to the right ventricle.

Fig. 5 Relative changes calculated in comparison to pathological conditions (EesR Ees$_{RIGHT}$=0.3; 0.5 and 0.8 mmHg/ml) for different type of RVAD connection and different rotational speed. For each values of Ees$_{RIGHT}$, the relative change was calculated when the RVAD was connected in parallel and “in series” mode. The left upper (lower) panel shows the relative changes in the left ventricular end systolic (end diastolic) volume when the RVAD was connected in parallel to the right ventricle. The right upper (lower) panel shows the relative changes in the left ventricular end systolic (end diastolic) volume when the RVAD was connected in series to the right ventricle.

medRxiv preprint doi: https://doi.org/10.1101/2022.03.22.22272760; this version posted March 23, 2022. The copyright holder for this preprint (which was not certified by peer review) is the author/funder, who has granted medRxiv a license to display the preprint in perpetuity. All rights reserved. No reuse allowed without permission.

Fig. 6 Relative changes calculated in comparison to pathological conditions (EesR□Ees$_{RIGHT}$=0.3; 0.5 and 0.8 mmHg/ml) for different type of RVAD connection and different rotational speed. For each values of Ees$_{RIGHT}$, the relative change was calculated when the RVAD was connected in parallel and in series mode. The left (right) upper panel shows the relative changes in the right (left) atrium pressure-volume loop area when the RVAD was connected in parallel to the right ventricle. The left (right) lower panel shows the relative changes in the right (left) atrium pressure-volume loop area when the RVAD was connected in series to the right ventricle.

Fig. 7 Relative changes calculated in comparison to pathological conditions (EesR□Ees$_{RIGHT}$=0.3; 0.5 and 0.8 mmHg/ml) for different types of RVAD connection and different rotational speed. For each value of Ees$_{RIGHT}$, the relative change was calculated when the RVAD was connected in parallel and in series mode. The left (right) upper panel shows the relative changes in the total cardiac output (right ventricular flow output plus RVAD flow output) when the RVAD was connected in series (parallel) to the right ventricle. The left (right) lower panel shows the relative changes in the right ventricular flow output when the RVAD was connected in series (parallel) to the right ventricle.

Fig. 8 Screen output generated by CARDIOSIM© platform. The left (right) upper panel shows the left (right) ventricular pressure-volume loops when pathological conditions (Ees$_{RIGHT}$=0.3 mmHg/ml) (black line), in-parallel RVAD (pump rotational speed at 3000 rpm) (red line) and in-series

medRxiv preprint doi: https://doi.org/10.1101/2022.03.22.22272760; this version posted March 23, 2022. The copyright holder for this preprint (which was not certified by peer review) is the author/funder, who has granted medRxiv a license to display the preprint in perpetuity. All rights reserved. No reuse allowed without permission.

RVAD assistance (pump rotational speed at 3000 rpm) (blue line) were reproduced by the simulator, respectively. The left (right) lower panel shows the left (right) atrial pressure-volume loops reproduced by CARDIOSIM©.

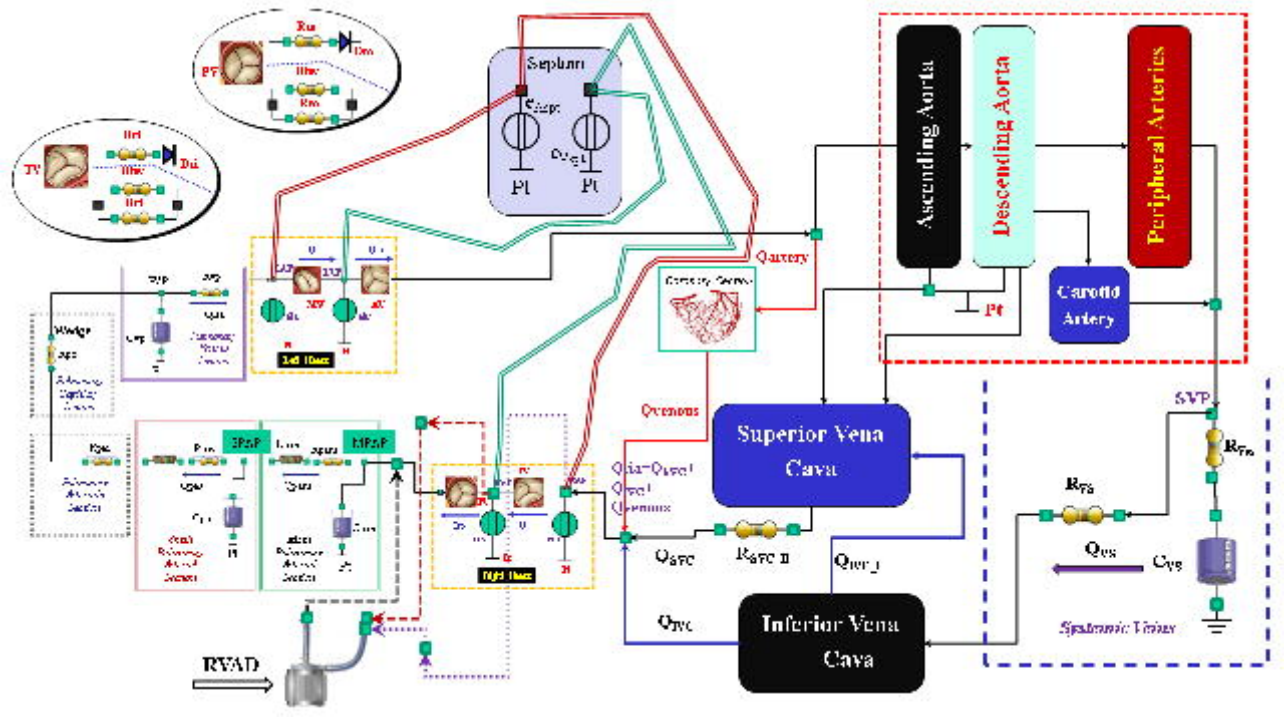

Septum
Pt
Pt
Ascending Aorta
Descending Aorta
Peripheral Arteries
Carotid Artery
Pt
Qartery
Qvenous
Superior Vena Cava
Inferior Vena Cava
SVP
Systemic Veins
RVAD

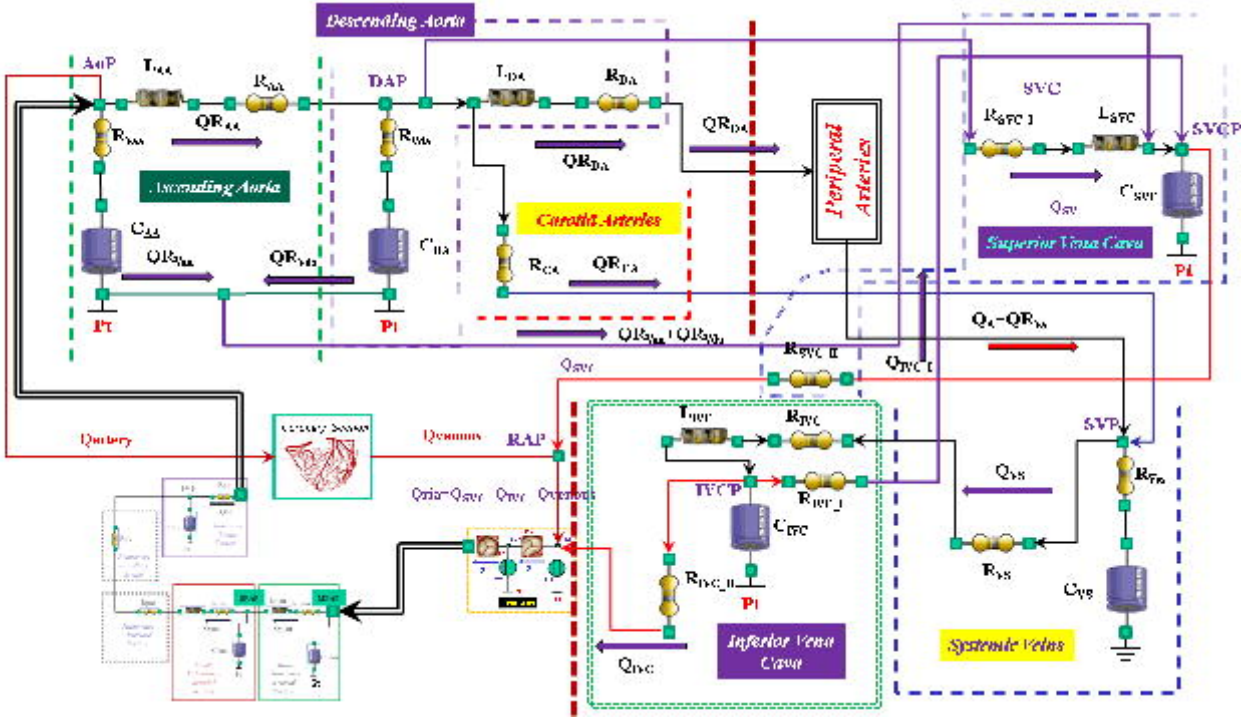
Descending Aorta
AoP
DAP
Ascending Aorta
Carotid Arteries
Peripheral Arteries
SVC
Superior Vena Cava
SVCP
PI
Systemic Veins
SVP
Inferior Vena Cava
IVCP
RAP

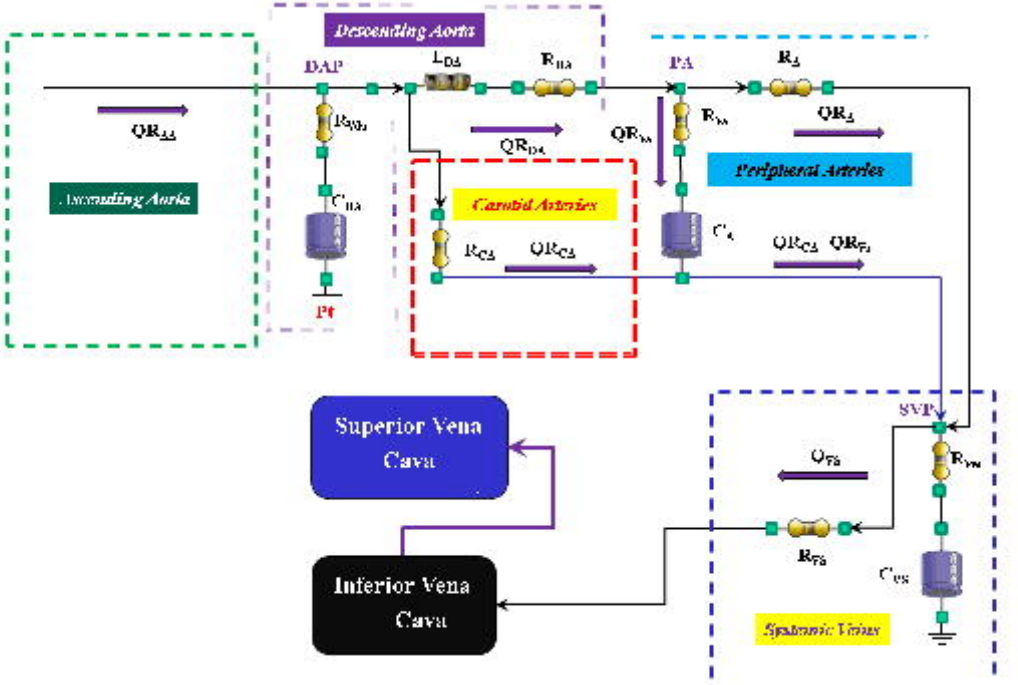
Descending Aorta
DAP
L_{DA}
R_{DA}
PA
R_A
QR_{AA}
R_{WD}
QR_{DA}
QR_{WA}
R_{WA}
QR_A
Ascending Aorta
C_{DA}
Carotid Arteries
Peripheral Arteries
R_{CA}
QR_{CA}
C_A
QR_{CA} QR_{PA}
Pf
Superior Vena Cava
SVP
R_{VM}
Q_{PA}
R_{PA}
Inferior Vena Cava
C_{VS}
Systemic Veins

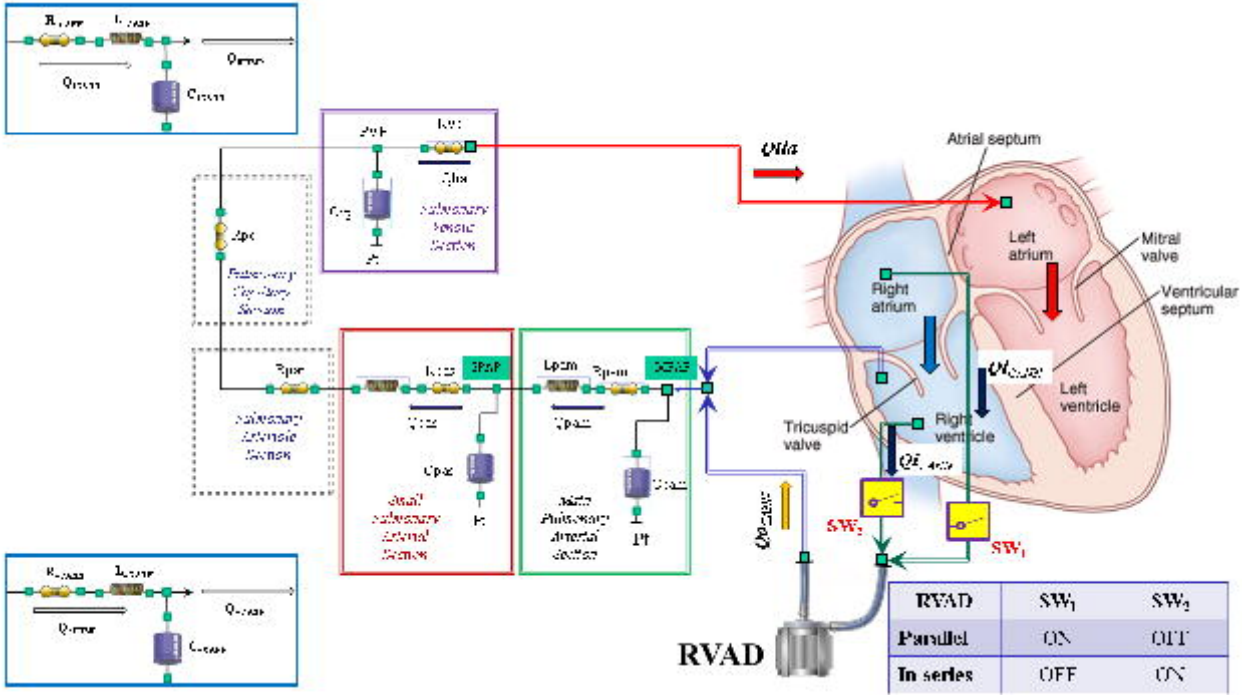

RVAD	SW_1	SW_2
Parallel	ON	OFF
In series	OFF	ON

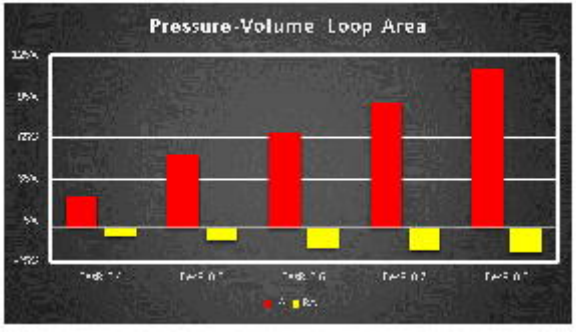
Pressure-Volume Loop Area

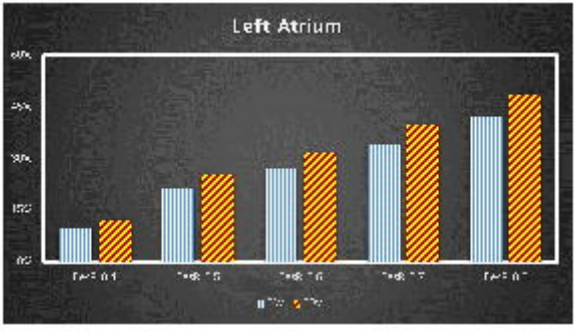
Left Atrium

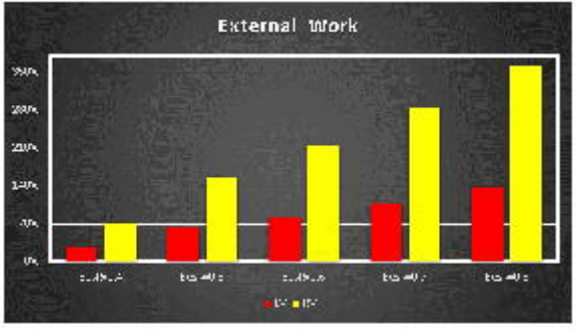
External Work

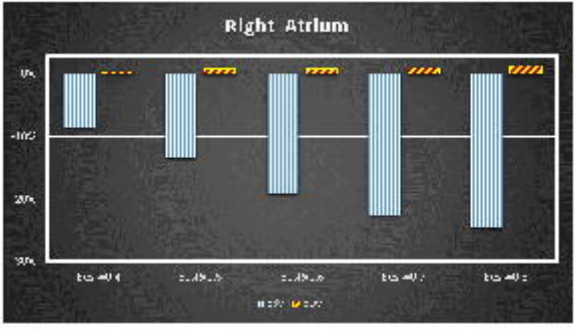
Right Atrium

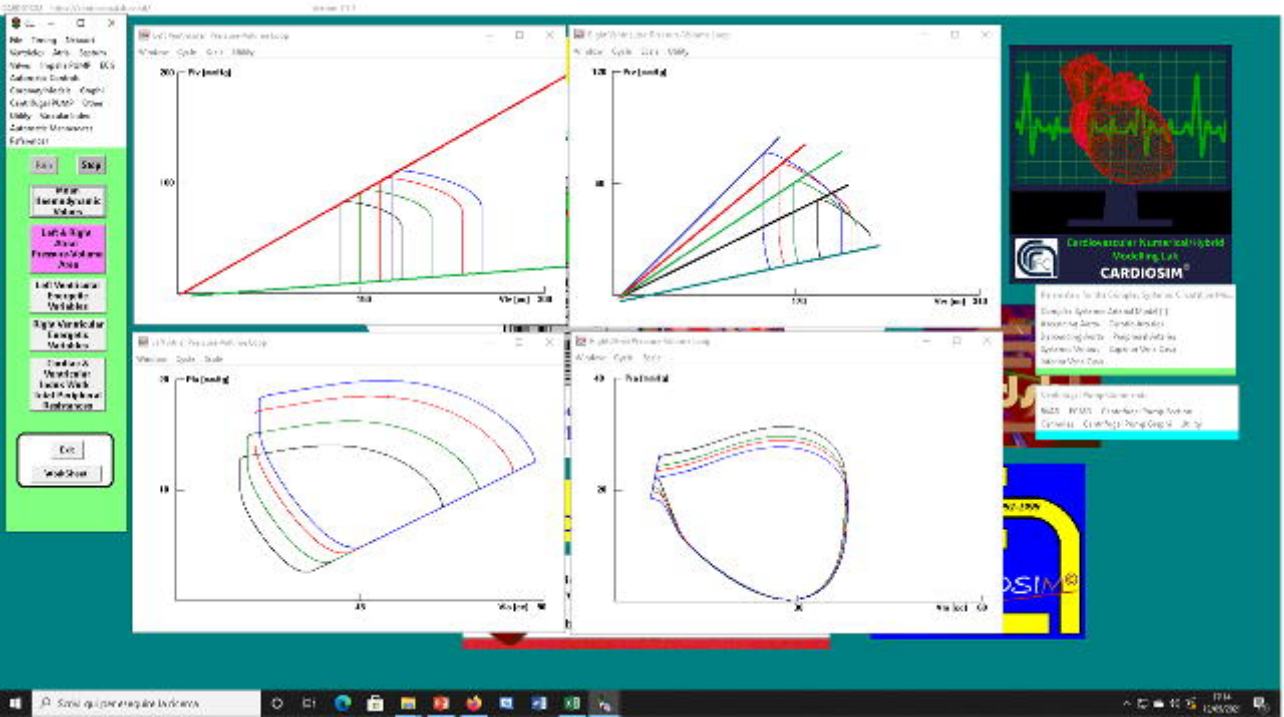
Cardiovascular Numerical Hybrid Modelling Lab
CARDIOSIM®

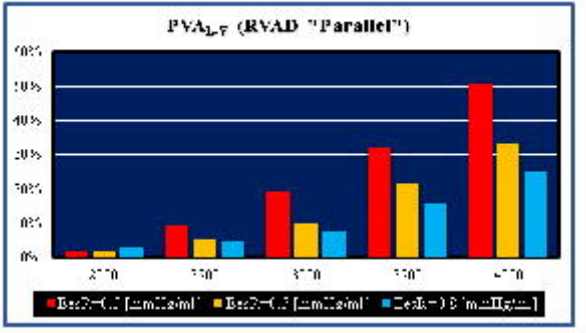
PVA$_{L,V}$ (RVAD "Parallel")

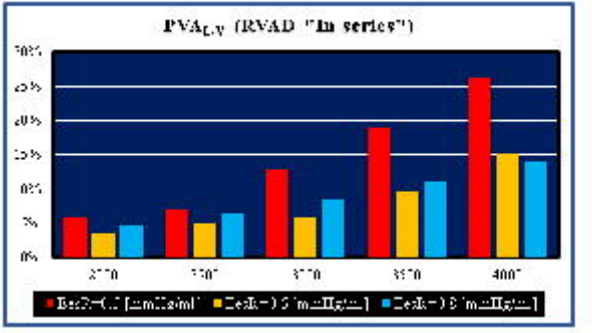
PVA$_{L,V}$ (RVAD "In series")

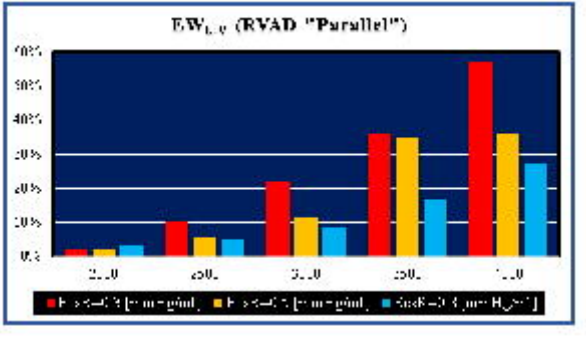
EW$_{L,V}$ (RVAD "Parallel")

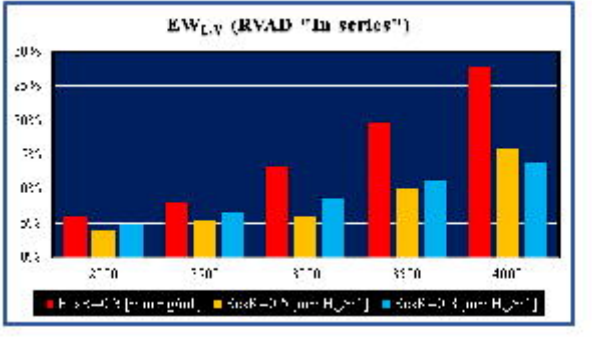
EW$_{L,V}$ (RVAD "In series")

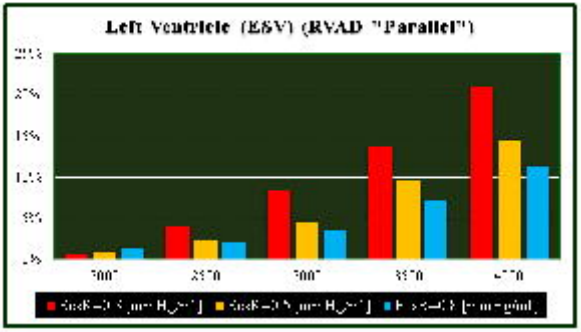
Left Ventricle (ESV) (RVAD "Parallel")

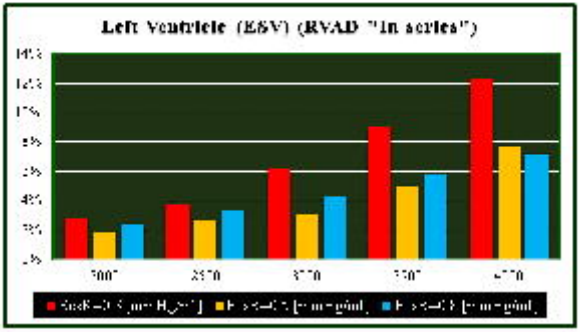
Left Ventricle (ESV) (RVAD "In series")

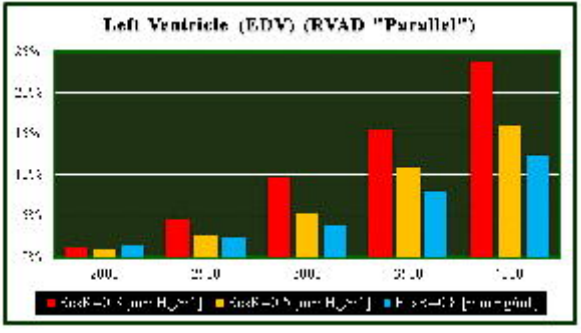
Left Ventricle (EDV) (RVAD "Parallel")

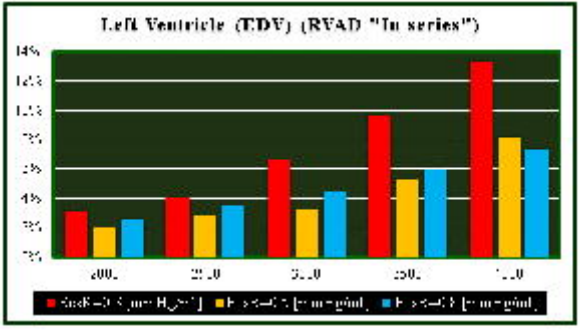
Left Ventricle (EDV) (RVAD "In series")

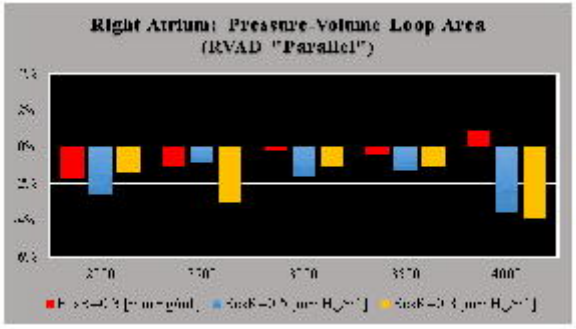
Right Atrium: Pressure-Volume Loop Area
(RVAD "Parallel")

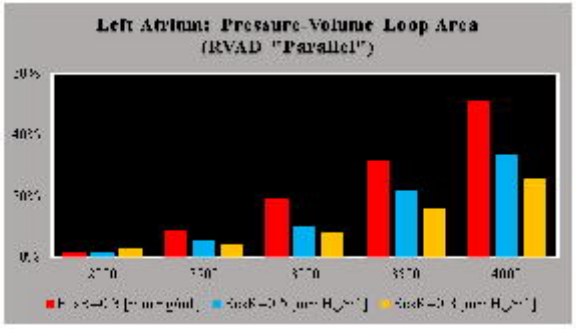
Left Atrium: Pressure-Volume Loop Area
(RVAD "Parallel")

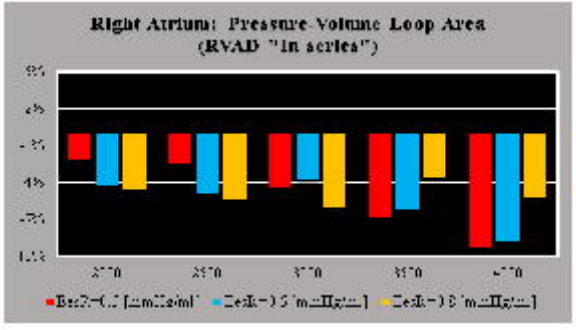
Right Atrium: Pressure-Volume Loop Area
(RVAD "In series")

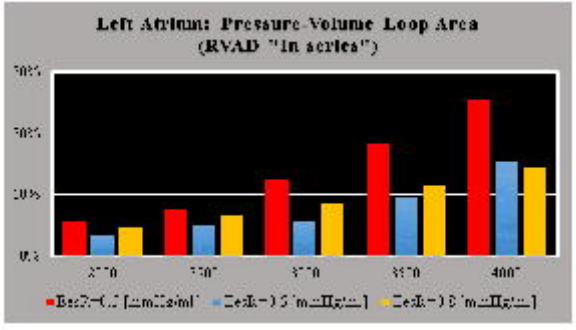
Left Atrium: Pressure-Volume Loop Area
(RVAD "In series")

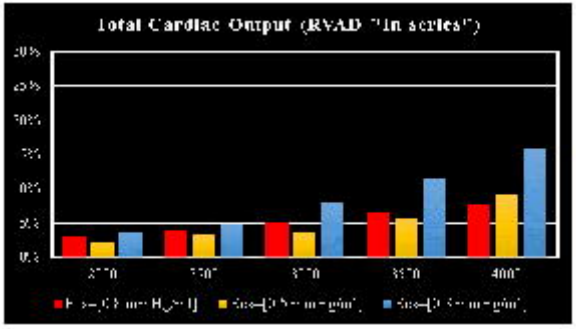
Total Cardiac Output (RVAD "In series")

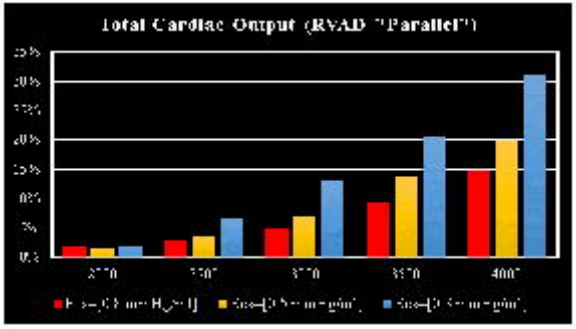
Total Cardiac Output (RVAD "Parallel")

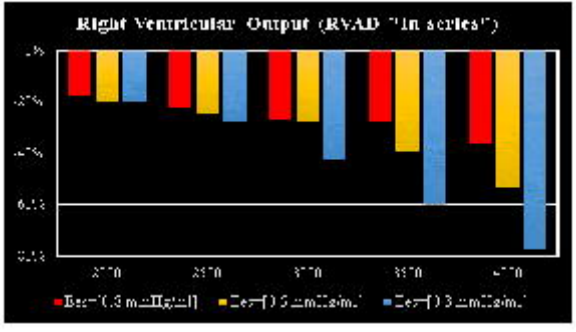
Right Ventricular Output (RVAD "In series")

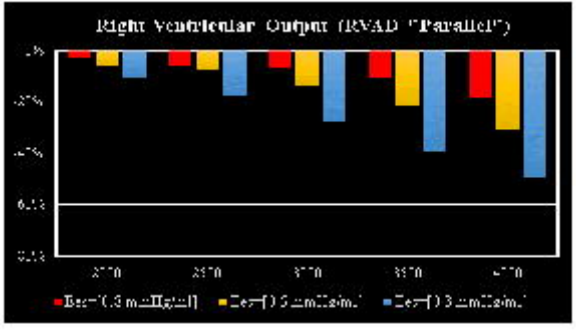
Right Ventricular Output (RVAD "Parallel")

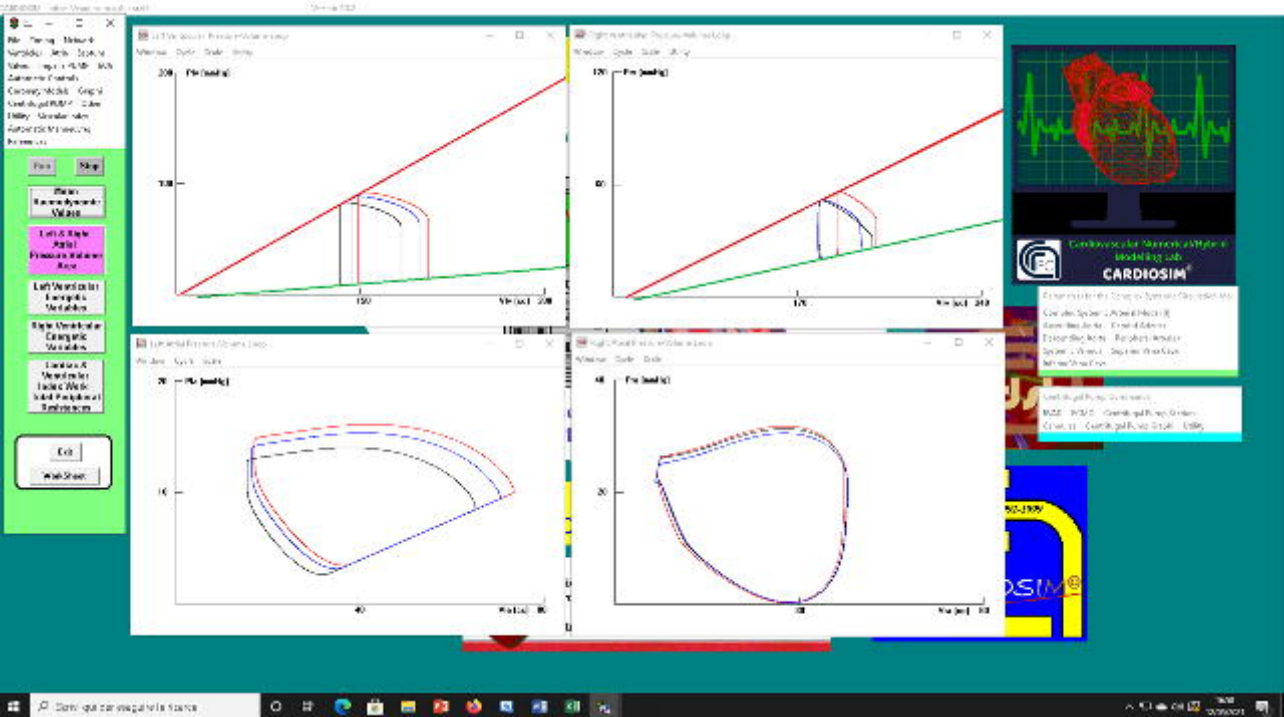
Cardiovascular Numerical Hybrid Modeling Lab
CARDIOSIM®